# NEW COREFLOOD SIMULATOR BASED ON INDEPENDENT TREATMENT OF IN-SITU SATURATION AND PRESSURE DATA

David J Element and Stephen G Goodyear
AEA Technology plc
Winfrith, Dorchester, Dorset, DT2 8ZE, United Kingdom

## ABSTRACT

When capillary pressure is important water/oil and gas/oil displacement tests need to be interpreted carefully to establish the underlying relative permeability, since the JBN method will under estimate oil recovery and artificially suppress relative permeabilities. Previous work used a recasting of the Darcy flow equations to develop a method for interpreting displacement tests by direct processing of saturation data. These recast equations have now been used as the basis for a new coreflood simulator, which allows pressure drop and saturation data to be analysed separately. This approach has a number of advantages over conventional core flood simulators: the regression problem can be decoupled into three independent steps, the actual observed saturation history at the core outlet can be used as a boundary condition, and the interpreted fractional flow curve is independent of any assumptions about the phase pressure that is measured at the outlet. Regression to the observed data is achieved using a genetic algorithm. Analysis of saturation data can be made for the full length of the core or for data from defined subsections. This can be valuable when considering composite cores or when parts of the core are significantly affected by heterogeneity.

The simulator is used to interpret results from a four rate waterflood on a carbonate core, to obtain relative permeability curves. The shape of the capillary pressure curve was also derived, however the cross-over saturation is not uniquely defined on the basis of the pressure measurements made, which were not phase selective. The simulator has also been used in a coreflood design mode, to select the minimum number of flow rate steps (including optimal selection of the individual rates) needed to derive reliable relative permeability curves, without unnecessarily complicating the laboratory flooding sequence.

## INTRODUCTION

Laboratory special core analysis (SCAL) water or gas flooding studies to determine relative permeabilities need to be performed in such a way that they are representative of reservoir conditions. The importance of preparation methods to condition the core to an appropriate initial water saturation and wettability, together with the choice of fluids and flooding rates, are increasingly recognised as key elements of definitive SCAL programmes. The results from core floods need to be interpreted to determine relative permeabilities. The conventional Johnson Bossler and Naumann (JBN) interpretation

method [1] uses oil production and pressure drop data to calculate relative permeabilities, assuming that the influence of capillary pressure on the displacement can be neglected. However, where capillary pressure is important, as illustrated by the waterflood data in Figure 1, the JBN method can give misleading results, and more sophisticated interpretation methods are required.

Current best practice uses simulation methods to include the effects of capillary pressure. Separately measured static capillary pressure and/or limited in-situ saturation data are used to constrain regression methods to fit to production and pressure drop data [2-5]. Where an independent measurement of capillary pressure is made on a second core, it may be difficult to ensure that it is representative of the original reservoir rate displacement test. The regression problem is made difficult by the large number of strongly coupled parameters that characterise the relative permeabilities and capillary pressure. Experience shows that results often fail to capture the development of in-situ saturation data satisfactorily, especially at the core outlet where a fixed saturation (corresponding to the conventional zero capillary pressure boundary condition) may not be observed, Figure 1.

Previous work [6] showed that saturation and pressure drop data can be analysed separately. Fractional flow data can be extracted from the saturation data independent of any boundary condition assumptions. Mobility data can be extracted from the pressure drop data, but this is always subject to some degree of uncertainty because of the ambiguity in how pressures measured in the inlet and outlet lines are related to phase pressures in the core at the inlet and outlet face. This paper describes the implementation of these ideas in a new core flood simulator and the application of the method to a multi-rate water flood and to the design of core flooding sequences.

## FORMULATION OF BASIC EQUATIONS

A full solution and regression method for core flooding has been developed for water/oil and gas/oil displacements including the effects of gravity. In this paper, to simplify the analysis and to focus on the way different parts of the multi-phase flow functions can be related to the saturation data, we only discuss the case of waterflooding in which gravity forces are ignored.

It is assumed that the core can be treated as a homogeneous one dimensional system with a uniform immobile initial water saturation. The starting point for the new interpretation methods is Darcy's law, where the phase velocities are expressed according to:

$$U_\alpha = -k\lambda_\alpha \frac{\partial p_\alpha}{\partial z} \tag{1}$$

where $\lambda_w$ and $\lambda_o$ are the water and oil phase mobilities respectively, defined by:

$$\lambda_\alpha = k_{r\alpha} / \mu_\alpha \tag{2}$$

and the water/oil capillary pressure $p_{cw}(S_w)$ is defined in the standard convention by:

$$p_{cw}(S_w) = p_o(S_w) - p_w(S_w)\,. \tag{3}$$

Coreflooding sequences are normally designed so that any change in the fluid volumes due to the pressure drop along the core can be neglected so that the total Darcy velocity $U(t)$ is known. This allows the Darcy equation for each phase to be re-cast to separate the pressure and fractional flow terms.

**Saturation Equation**

The pressure independent equation forms an extension of the familiar fractional flow equation with a convective and dispersive term:

$$U_o = U(t) f_o(S_w) + k d_{cpw}(S_w) \frac{\partial S_w}{\partial z}\,. \tag{4}$$

$f_o$ is the conventional viscous dominated fractional flow curve:

$$f_o(S_w) = \frac{\lambda_o}{\lambda_w + \lambda_o}\,. \tag{5}$$

The capillary dispersion rate function $d_{cpw}$ is given by

$$d_{cpw}(S_w) = -\frac{\lambda_o \lambda_w}{\lambda_w + \lambda_o} \frac{dp_{cw}}{dS_w}\,, \tag{6}$$

which corresponds to the counter-current flow term associated with capillary imbibition. Using a saturation equation, decoupled from the pressure in this way, is the basis of the fractional flow equation first introduced by Leverett for immiscible displacements [7].

**Pressure Equation**

Since pressure data is only known at a few positions, usually just at the ends of the core, a more global form of the pressure equation has to be formulated to make use of this information. One of the difficulties encountered here is a possible ambiguity in how pressures measured in the inlet and outlet lines are related to phase pressures in the core at the inlet and outlet face (since the oil and water phase pressures are different by the capillary pressure). It is reasonable to assume that the inlet pressure corresponds to the water phase pressure at the inlet face of the core and that at some point after water breakthrough the outlet pressure corresponds to the water phase pressure at the outlet face of the core. In this case the pressure difference can be determined by re-arranging and integrating Equation 1 along the length of the core:

$$\Delta p(t) = \int_0^L \frac{U_w(z,t)}{k \lambda_w(S(z,t))} dz\,. \tag{7}$$

## OVERALL ANALYSIS STRATEGY

This section describes the overall regression strategy and the way the problem is split into three separate stages. The oil Darcy velocity (Equation 4) can be written as:

$$U_o = U(t) f_o(S_w) \left( 1 + \frac{k}{U(t)} E_w(S_w) \frac{\partial S_w}{\partial z} \right) \tag{8}$$

where the end effect function $E_w$ is related to $f_o$ and $d_{cpw}$ through:

$$d_{cpw} = E_w f_o \tag{9}$$

During a multi-rate displacement the saturations will approach a pseudo-steady distribution at the end of each flow rate period where the viscous and capillary forces are balanced. At this point the oil Darcy velocity is zero, and from Equation 8

$$E_w(S_w) = -U(t)\left(k\frac{\partial S_w}{\partial z}\right)^{-1}, \tag{10}$$

so that $E_w$ is determined by the saturation distributions at the pseudo-steady states.

The overall solution strategy is to work with the multiphase flow functions defined in terms of $f_o$, $E_w$ and $\lambda_w$. This has a significant mathematical benefit, because it effectively "diagonalises" the functions, so that in principle the regression for each function can be undertaken in separate stages, Figure 2. In the first stage the pressure data is analysed to determine $\lambda_w$, using the measured saturation profiles. Secondly the pseudo-steady states can be analysed using Equation 10, to determine $E_w$ for the saturations present. Finally the dynamic saturations are considered and a regression performed to obtain $f_o$ (and $E_w$ for saturations not present in the pseudo-steady state saturation distributions). The functions $f_o$, $E_w$ and $\lambda_w$ are then deconvoluted using Equations 5, 6 and 9 to obtain $k_{ro}$, $k_{rw}$ and $p'_{cw}$.

In practice Stage 2 and 3 may be combined into a single regression, since it may not be possible to obtain good estimates of the pseudo-steady state saturation distributions corresponding to each flow rate bump, if oil is still being produced and the data requires significant extrapolation. In this case, analysis of the saturation data at Stage 2 may be used to precondition this combined regression. The overall regression strategy described here has also been used for the full core flood equations including gravity terms.

**Benefits of Chosen Multi-Phase Parameterisation**

Separation of the saturation and pressure equation allows the uncertainty associated with each data category to be correctly assigned to the underlying multi-phase flow function. For pressure drop data uncertainty arises from scatter in the data itself (which in reservoir condition tests may be relatively large compared to the saturation data) and from the intrinsic uncertainty in whether it is the oil or water phase pressure that is being measured around the time of water breakthrough. This uncertainty manifests itself through the water mobility. Uncertainty in the saturation data feeds through into the fractional flow curve, which because of the explicit representation of the outlet saturation history is free from boundary condition assumptions. In this way the most important function determining recovery efficiency is determined with the minimum uncertainty.

The explicit use of the observed saturation history at the outlet allows subregions of a core to be modelled. For example, single plugs within a composite can be modelled, or regions of unrepresentative behaviour excluded. The saturation history at the downstream

end of the region is used as the outlet condition and the inlet boundary condition is taken as the fractional flow of water into the region, which can be directly calculated from the time evolution of the upstream saturation profiles.

## SOLUTION OF PRESSURE EQUATION

Solution of the pressure equation (Equation 7) requires the water mobility to be determined. The solution algorithm is based on a least squares regression on the pressure equation, using the measured in-situ saturation profiles and varying a parameterised form of the water mobility function.

## SOLUTION OF SATURATION EQUATION

Equation (8) is combined with the mass conservation equation and solved numerically with a conventional implicit finite difference method, using single-point upstream weighting for the flux functions. The inlet boundary condition is defined by the injected fractional flow of water and the outlet boundary condition is chosen to be the observed outlet saturation history, $S_w^{out}(t)$, so that the oil flowrate at the outlet of the core is defined in terms of the outlet saturation gradient according to:

$$U_o^{out}(t) = U(t) f_o(S_w^{out}(t)) \left( 1 + \frac{k}{U(t)} E_w(S_w^{out}(t)) \frac{\partial S_w}{\partial z}\bigg|_{z=L} \right) \tag{11}$$

This differs from the conventional assumption that $p_{cw} = 0$, which has the effect of fixing the outlet saturation at one value. The boundary condition can give rise to an ill-posed problem, if the underlying multi-phase flow functions do not allow mobile water to reach the core outlet before the boundary saturation increases from $S_{wi}$. This problem is addressed by setting $S_w^{out} = S_{wi}$ until mobile water reaches the outlet of the core. When used in a regression mode, the multi-phase functions inevitably converge to be consistent with the imposed outlet saturation history.

### Genetic Algorithm

Genetic algorithms [8] provide a robust methodology for global, non-linear optimisation problems, using a randomised search method which emulates the principle of "survival of the fittest". The “unknown” parameters are divided into a number of genes, which together form a *chromosome*. An entire *population* of chromosomes is constructed, and for each chromosome an *objective function* is evaluated – this being a measure of how closely the chromosome represents the target solution. A set of new chromosomes is then constructed to form a completely new population (the next *generation*). Each chromosome in the next generation is formed by combining a pair of chromosomes (the *parents*) selected at random from the previous generation, in such a manner that chromosomes with the best objective function are more likely to be chosen than poorer chromosomes. The combination of parents’ genes to define a new offspring chromosome makes use of *gene-mating* and *gene-mutation* techniques. Over the course of a number of generations, chromosomes that give better solutions to the target solution should emerge,

as a result of the "survival of the fittest" principle. Genetic algorithms do not guarantee that the optimal solution is found, but will at least find a solution close to the optimal. Compared to some other optimisation techniques, genetic algorithms do not require the objective function to be continuous or differentiable, and are also not sensitive to the initial starting point for a regression.

A genetic algorithm has been combined with the coreflood simulator to create a regression capability so that the $f_o$ and $E_w$ curves can be optimised with respect to the experimental saturation data. The chromosome has two parts:

- the fractional flow curve, divided into individual segments, satisfying the constraint that the complete curve is monotonic, and bounded in the range [0,1].
- the end effect function, divided into small segments, subject only to the constraint that $E_w$ is positive.

The initial population of fractional flow curves is generated using Corey relative permeabilities with random Corey parameters. Figure 3 illustrates such a random set. For this first generation it is not necessary that any individual fractional flow curve should be close to the optimal solution. The initial set of $E_w$ curves is constructed using the pseudo-steady state saturation distributions (see discussion of Equation 10). For each pair of $f_o$ and $E_w$ curves, a coreflood simulation is run. The objective function for that simulation is based on an appropriate least squares error between simulated and measured saturation profiles. A population size of around 50-100 is usually adequate for core flood interpretation (which is consistent with the population size found to be suitable for a whole range of optimisation problems solved using genetic algorithms). Several hundred generations are typically required to converge to an "optimal" pair of $f_o$ and $E_w$ curves.

## VALIDATION OF METHODS

The method is validated on a multi-rate synthetic waterflood. Figure 4 plots the value of the objective function for the best solution in each generation, showing convergence as the regression continues. Since the core was set up to be homogeneous and the coreflood saturation values were free of any noise, the "optimal" solution could be expected to have an objective function of zero. In this analysis the genetic algorithm continued to converge ever-closer to the true solution, even after 700 complete generations. The "best" pair of $f_o$ and $E_w$ curves from the $700^{th}$ generation are compared to the true solutions in Figures 5 and 6, validating the performance of the regression techniques.

## ANALYSIS OF MULTI-RATE CARBONATE WATERFLOOD DATA

The new approach to core flood simulation has been applied to the interpretation of third party data from a multi-rate waterflood on a carbonate core. The core comprised a single plug 6 cm long, with a porosity of 29% and permeability of 14.8 md. The water flood was performed at four rates and the pressure drop and in-situ saturation distribution (at a 2mm resolution) were measured.

The pressure data provided had already been smoothed, although it would have been preferable to work with the underlying raw data. The data was analysed in terms of the water mobility, assuming that after water breakthrough the outlet pressure corresponds to the water phase. Figure 7 shows the comparison between the modelled pressure difference and the supplied data. The modelled pressures are not smooth, because they are calculated based on the measured saturation profiles which are affected by local heterogeneity and statistical noise. Figure 8 shows the interpreted $k_{rw}$ curve, which as expected lies above the JBN interpretation and the "end point" $k_{rw}$ values, which are still influenced by capillary end effects.

The saturation data was reviewed and it was found that the inlet region of the core had higher initial water saturations than the rest of the plug. The analysis method allows sub-regions of the core to be analysed. The first 2 cm of the saturation profiles were excluded from the analysis, along with the last two saturation points, as it was considered that these were too close to the end of the core to be fully reliable, Figure 9. The full saturation data set is shown in Figure 1. The saturation at the downstream end of the selected region was used as the outlet boundary condition for the simulation regression. Quality checks of the saturation data indicate mass balance problems at the start of the flood, since the rate of recovery from the core exceeds the quoted flood rate. The regression was performed using the nominal rates, which means there is a mismatch with the early pre-breakthrough data, as shown in the match to the oil production data in Figure 10. Example matches to the in-situ saturation data are shown in Figure 11. The JBN and simulation derived fractional flow curves are shown in Figure 12. The predicted recovery from the simulation derived fractional flow curve is compared with the results of the core flood in Figure 10, showing that a significantly better recovery performance would be expected in the reservoir. The final interpreted water and oil relative permeability curves are shown in Figure 13.

The derivative of the capillary pressure is known from the multiphase flow functions deduced from the regression, and so $p_{cw}$ is defined to within a constant. Although the constant cannot be determined uniquely from the data, the saturation at which $p_{cw} = 0$ must lie between the initial water saturation and the water saturation measured at the core outlet at the end of the low rate waterflood (since this corresponds to a partially forced imbibition). The shape of the capillary pressure curve is shown in Figure 14. If phase selective pressure transducers were available [9] the ambiguity in interpretation of the pressure data would be removed, allowing the capillary pressure curve to be fully determined.

## OPTIMISATION OF CORE FLOOD SEQUENCE DESIGN

The simulation regression tool has been used to assess the impact of core flood sequence design on the quality of the interpreted relative permeabilities. Using the same multi-phase functions as in the earlier validation test, synthetic in-situ saturation profiles have

been generated by adding a random error to each data point (representing the error from counting statistics) and a systematic spatial variation in saturation with is scaled by the water saturation value (representing the effect of local heterogeneity). The core was 8cm in length and saturation data were constructed at a spatial resolution of 3mm with a minimum total scan time of 360s and a random error with a standard deviation of 0.75 saturation units. This is representative of what can be achieved with X-ray attenuation measuring techniques. In the first set two flow rates were used, 4 and 400 ml/h, while in the second set a multi-rate sequence was followed, 4, 20, 100 and 400 ml/h. Figure 15 shows the saturation profiles for the four-rate waterflood. The profiles for the two-rate waterflood are effectively the same as these, except that the 20 and 100 ml/h profiles are absent.

The saturation profiles were interpreted using the regression tool and very good fits were found to the saturation profiles in both cases, as is illustrated by the quality of the match to the effluent production curves constructed from the saturation profiles, Figure 16. However, the interpreted fractional flow curves show significant differences, Figure 17, with the fractional flow curve from the two-rate data giving significantly earlier water breakthrough, Figure 18, than predicted by the underlying fractional flow curve. The two-rate data produces a poorer result because there is no overlap in the saturation profiles between the low and high rates, leaving a data-gap in which there is no information to constrain the regression. Using a larger number of rate steps ensures that there is a good overlap between the range of saturations present in each rate step. In this example the maximum increase in rate was limited to a factor of five, which ensures that saturations in the pseudo-steady condition at the end of each flow rate bump should overlap for at least 20% of the core length.

## CONCLUSIONS

1. The equations for coreflood simulation have been reformulated in terms of a “natural parameterisation” of the multi-phase functions each with a clear physical meaning. This effectively “diagonalises” the functions, so that in principle the regression for each function can be undertaken in separate stages.
2. The evolution of the in-situ saturations is determined by only two independent functions, and a new core flood simulator has been developed based on this formulation which allows the observed outlet saturation to be used as the boundary condition, rather than forcing a fixed saturation.
3. A genetic algorithm has been developed and coupled to the simulator to allow regression analysis of in-situ saturation profiles.
4. A four rate waterflood on a carbonate plug was analysed with the new methods to determine relative permeabilities and the shape of the capillary pressure curve. By focussing on a sub-region of the core, it was possible to avoid a region with a non-uniform initial water saturation.

5. The use of more than one flow-rate bump significantly improves the accuracy of the interpreted fractional flow curve and it is recommended that the difference in rates between each bump should be less than a factor of five.

## NOMENCLATURE

| | |
|---|---|
| $d_{cpw}$ | capillary dispersion rate [$s^{-1}$] |
| $E_w$ | end effect function [$s^{-1}$] |
| $f_o$ | viscous dominated fractional flow [-] |
| $k$ | permeability [$m^2$] |
| $k_{r\alpha}$ | relative permeability of phase $\alpha$ [-] |
| $L$ | length of core [m] |
| $p_{cw}$ | water/oil capillary pressure [Pa] |
| $p_\alpha$ | pressure of phase $\alpha$ [Pa] |
| $S_\alpha(z,t)$ | saturation of phase $\alpha$ [-] |
| $S_w^{out}(t)$ | outlet saturation at time t [-] |
| $t$ | time [s] |
| $U(t)$ | total Darcy velocity [m $s^{-1}$] |
| $U_\alpha$ | Darcy velocity of phase $\alpha$ [m $s^{-1}$] |
| $z$ | distance from core inlet [m] |

Greek:

| | |
|---|---|
| $\Delta p$ | core pressure drop [Pa] |
| $\lambda_\alpha$ | mobility of phase $\alpha$ [$Pa^{-1}s^{-1}$] |
| $\mu_\alpha$ | viscosity of phase $\alpha$ [Pa s] |

Subscripts:

| | |
|---|---|
| $\alpha$ | phase label |
| $o$ | oil phase |
| $w$ | water phase |

## REFERENCES


1. Johnson, E.F., Bossler D.P. and Naumann, V.O., "Calculation of Relative Permeability from Displacement Experiments", *Trans., AIME* (1959), 370-72.
2. Richmond, P.C. and Watson, A.T., "Estimation of Multiphase Flow Functions from Displacement Experiments", *SPE Reservoir Engineering*, Feb 1990, 121-27.
3. Chardaire-Riviere, C., Chavent, G., Jaffre, J. and Liu J. and Bourbiaux, B.J., "Simultaneous Estimation of Relative Permeabilities and Capillary Pressure", *SPE Formation Evaluation*, (Dec 1992), pp283-289.
4. Mejia, G.M., Mohanty K.K., and Watson, A.T., "Use of In-Situ Saturation Data in Estimation of Two-Phase Flow Functions in Porous Media", *Journal of Petroleum Science and Engineering* (1995) **12** pp233-245.
5. Helset H.M., Nordtvedt J.E., Skjaeveland S.M. and Virnovsky G.A., "Relative Permeabilities from Displacement Experiments with Full Account for Capillary Pressure", *SPE Reservoir Evaluation & Engineering*, April 1998, pp92-98 (SPE 36684).
6. Goodfield, M., Goodyear, S.G., and Townsley, P.H., "New Coreflood Interpretation Method for relative Permeabilities Based on Direct Processing of In-Situ Saturation Data", SPE 71490, presented at Annual Technical Conference and Exhibition, New Orleans, LA, 30 September-3 October 2001.
7. Leverett, J.S., "Capillary Behaviour in Porous Solids", Trans. AIME 142, pp152-169.
8. Man, K.F., Tang, K.S. and Kwong, S. "Genetic Algorithms". Springer-Verlag, London, 1999.
9. van Wunnik, J.N.M., Oedai, S, and Masalmeh, S., "Capillary Pressure Probe for SCAL Applications", SCA-9908, 1999 Society of Core Analysts International Symposium, Golden, 1-4 August.

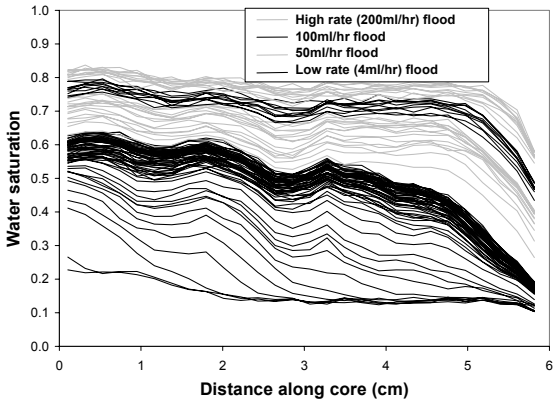


**Figure 1: Saturation profiles from multi-rate waterflood showing end effects and increasing outlet saturation with time**

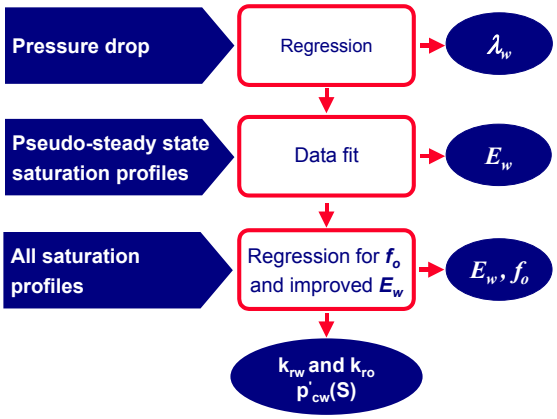


**Figure 2: Schematic diagram showing three independent stages in regression analysis**

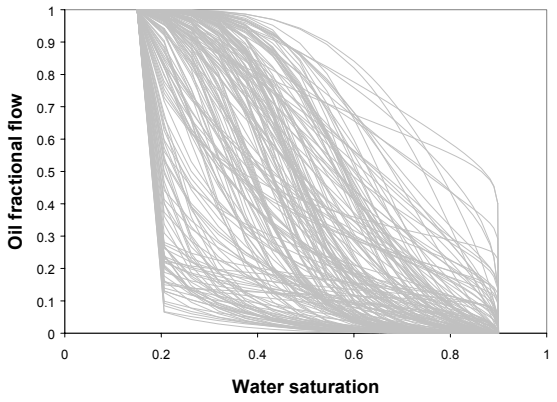


**Figure 3: Population of fractional flow curves at start of regression to saturation data from validation case**

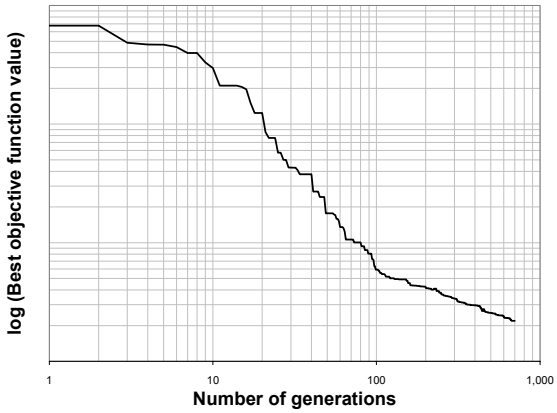


**Figure 4: Evolution of objective function in regression to saturation data from validation case**

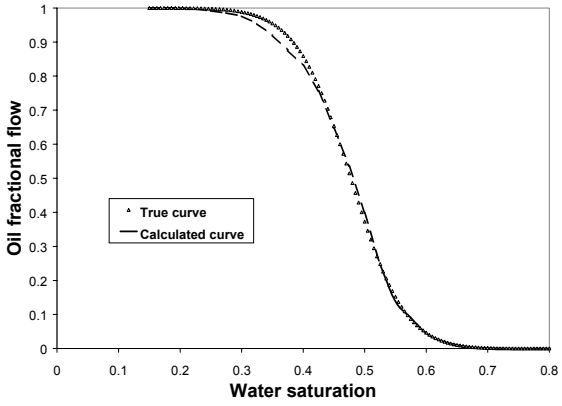


**Figure 5: Final oil fractional flow curve derived from regression, compared to underlying curve in validation case**

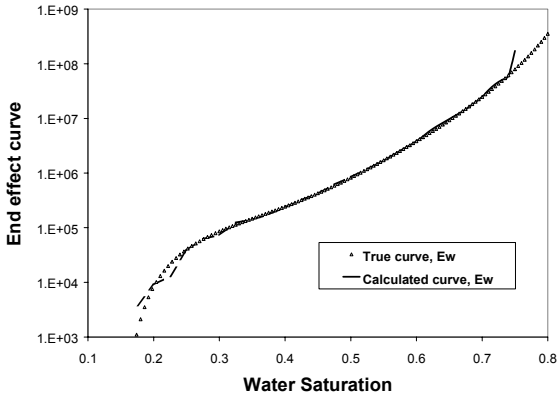


**Figure 6: Final end effect function $E_w$ derived from regression, compared to underlying curve in validation case**

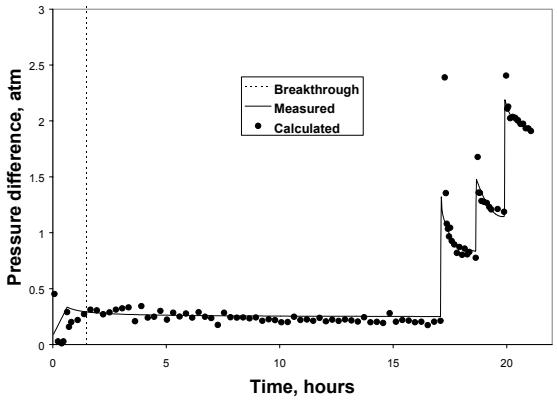


**Figure 7: Match to pressure drop data from multi-rate carbonate waterflood**

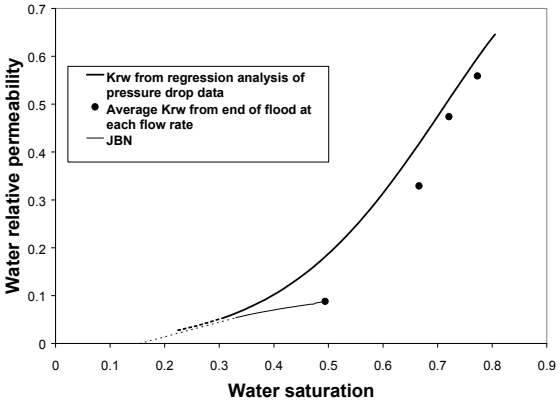


**Figure 8: Water relative permeability curve from regression analysis of multi-rate carbonate waterflood data**

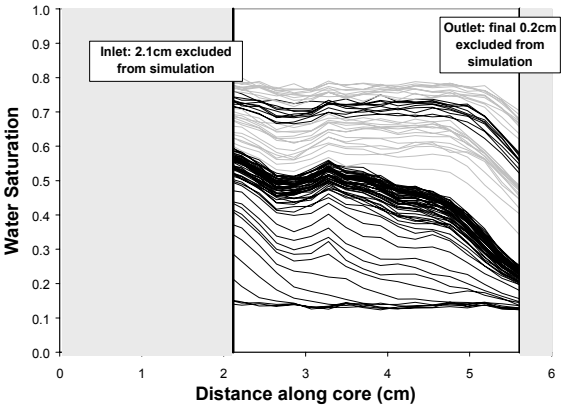


**Figure 9: Third party multi-rate carbonate waterflood saturation profiles showing selected analysis region**

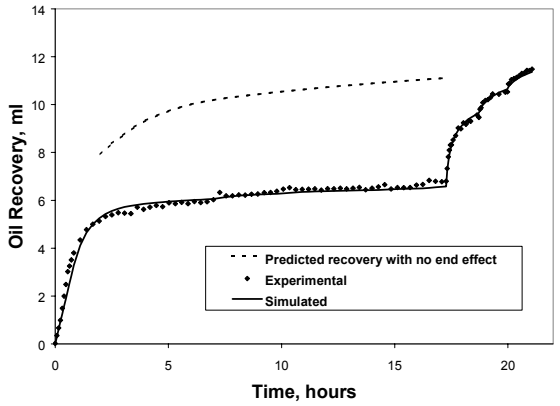


**Figure 10: Match to effluent profile of multi-rate carbonate waterflood, with predicted production without end effect**

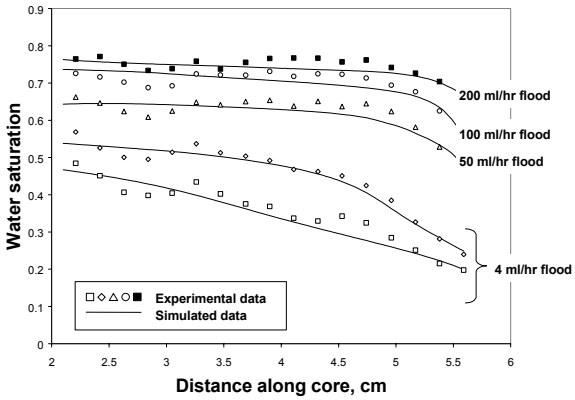


**Figure 11: Selected matches to in-situ saturation profiles for multi-rate carbonate waterflood**

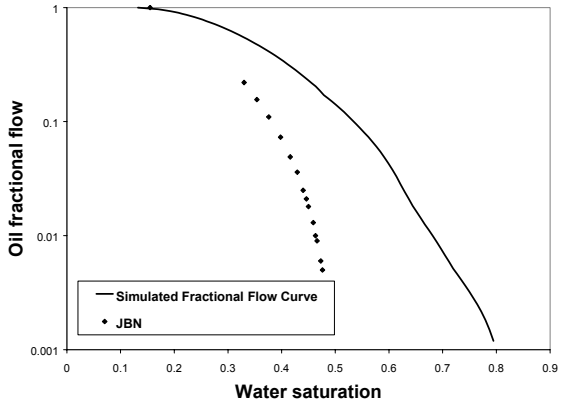


**Figure 12: Oil fractional flow curve from regression compared to JBN result for multi-rate carbonate waterflood**

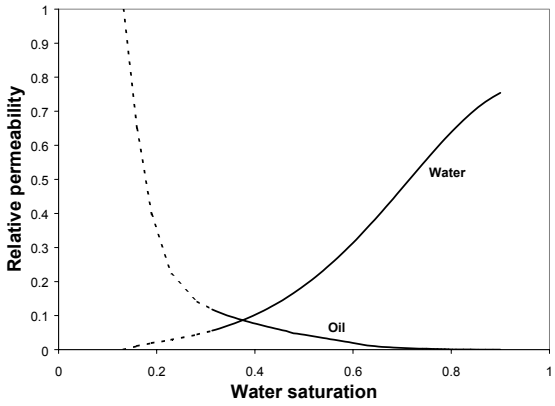


**Figure 13: Waterflood oil and water relative permeability curves for multi-rate carbonate waterflood**

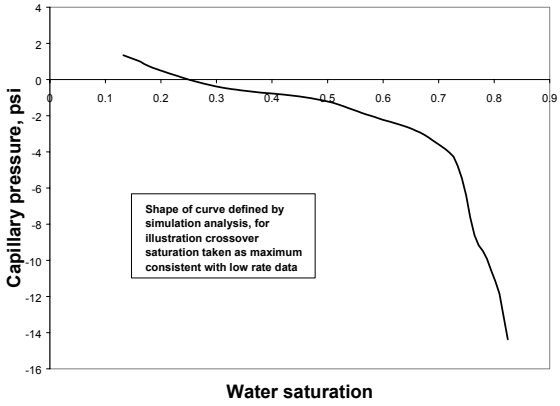


**Figure 14: Inferred shape of capillary pressure curve for result for multi-rate carbonate**

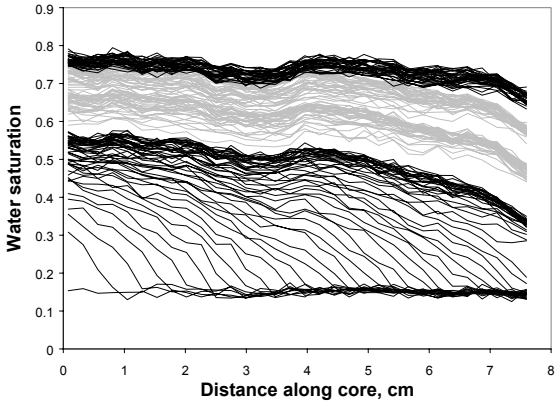


**Figure 15: Saturation profiles for synthetic four-rate waterflood**

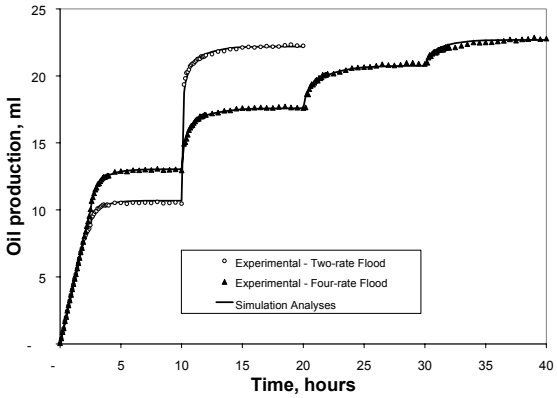


**Figure 16: Fit to two-rate and four-rate oil production curves for synthetic waterflood examples**

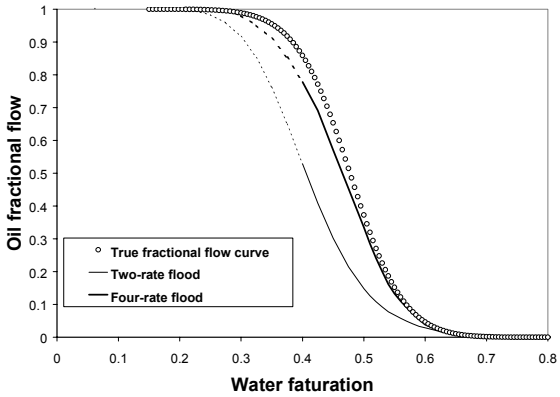


**Figure 17: Fractional flow curves obtained by regression to two-rate and four-rate synthetic waterflood data, compared to underlying curve**

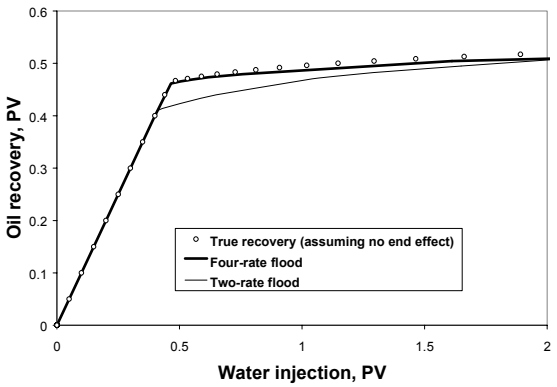


**Figure 18: Predicted oil recovery based on two-rate and four-rate waterflood interpretations, compared to underlying result**